

# PRETREATMENT ULTRASOUND-BASED RADIOMICS NOMOGRAM FOR PREDICTING PATHOLOGICAL COMPLETE RESPONSE TO NEOADJUVANT CHEMOTHERAPY IN HER2-POSITIVE BREAST CANCER

FeiFei Shan<sup>1</sup>, JunQi Sun<sup>2\*</sup>, Wei Zhou<sup>2</sup>, ChengYuan Zheng<sup>2</sup>

<sup>1</sup>Department of Ultrasound, Affiliated Yuebei People's Hospital of Shan University, Shaoguan 512026, Guangdong, China.

<sup>2</sup>Department of Radiology, Affiliated Yuebei People's Hospital of Shan University, Shaoguan 512026, Guangdong, China.

\*Corresponding Author: JunQi Sun

**Abstract:** Background: Accurately predicting pathological complete response (PCR) to neoadjuvant chemotherapy (NAC) in patients with human epidermal growth factor receptor 2 (HER2)-positive breast cancer is crucial for tailoring individualized treatment strategies. This study seeks to develop and validate a radiomics-based nomogram utilizing pretreatment ultrasound (US) data to predict PCR on an individual basis. Methods: In this retrospective analysis, patients diagnosed with HER2-positive breast cancer who underwent NAC were included and randomly assigned to either a training cohort (70%) or a validation cohort (30%) between January 2020 and December 2024. Radiomics features were extracted from the entire tumor volume as delineated on pretreatment US images. Feature selection was conducted using a combination of stability analysis, the Least Absolute Shrinkage and Selection Operator (LASSO) to establish a comprehensive radiomics signature (Rad-score). A predictive nomogram was then constructed by integrating the Rad-score with independent clinical predictors through multivariate logistic regression. The model's performance was assessed using the area under the receiver operating characteristic curve (AUC), calibration curves, and decision curve analysis (DCA). Results: The radiomics signature, consisting of 10 features derived from first-order statistics and texture matrices, exhibited significant predictive capability, achieving an area under the curve (AUC) of 0.705 in the validation cohort. The final nomogram, integrating the Rad-score, progesterone receptor (PR), demonstrated enhanced performance, with AUCs of 0.749 and 0.744 in the training and validation cohorts, respectively. Calibration curves and decision curve analyses confirmed the model's robust calibration and clinical applicability. Conclusion: The pretreatment ultrasonography-based radiomics nomogram offers a non-invasive and effective tool for the individualized prediction of pathological complete response (PCR) in HER2-positive breast cancer patients undergoing neoadjuvant chemotherapy (NAC), potentially aiding in the customization of therapeutic strategies.

**Keywords:** Breast cancer; HER2-Positive; Neoadjuvant chemotherapy; Ultrasonography; Radiomics; Machine learning

## 1 INTRODUCTION

Breast cancer remains a leading cause of cancer-related mortality among women globally [1]. The HER2-positive subtype, accounting for 15-20% of breast cancer cases, is distinguished by its aggressive tumor biology and historically poor prognosis. The incorporation of HER2-targeted therapies, such as trastuzumab and pertuzumab, into neoadjuvant chemotherapy (NAC) regimens has markedly enhanced pathological complete response (PCR) rates and survival outcomes [2-3]. Achieving PCR, defined as the absence of invasive cancer in both the breast and lymph nodes (ypT0/is ypN0), serves as a robust surrogate endpoint, strongly associated with excellent long-term event-free and overall survival [4].

Despite these advancements, the response to NAC remains variable, with PCR rates ranging from 40% to 65%, indicating that a significant proportion of patients experience the toxicity, cost, and delay of ineffective systemic therapy [5]. Presently, clinical assessment predominantly relies on postoperative histopathological evaluation, which is inherently retrospective. Conventional imaging techniques, such as ultrasound (US) and magnetic resonance imaging (MRI), primarily evaluate response based on changes in tumor size, which often lag behind molecular alterations and lack sufficient accuracy for early, individualized prediction [3-10]. Consequently, there is an urgent demand for reliable, non-invasive biomarkers that can predict treatment outcomes at the pretreatment stage.

Radiomics, a high-throughput computational approach, addresses this need by extracting and analyzing a comprehensive array of quantitative features from standard medical images. These features, which characterize tumor intensity, shape, and texture heterogeneity, can elucidate the underlying tumor phenotype and microenvironment—information that often remains imperceptible to the human eye [11-13]. Although much of the foundational research in breast cancer radiomics has focused on MRI, breast ultrasound (US) offers distinct practical advantages. It is widely accessible, cost-effective, non-ionizing, and serves as a cornerstone for breast cancer diagnosis and staging worldwide. Emerging evidence robustly supports the predictive value of US-based radiomics for assessing the response to neoadjuvant chemotherapy (NAC). Many research demonstrated that machine learning models

leveraging US radiomics features alongside clinical data could effectively predict NAC efficacy [14-18]. Moreover, dynamic models that incorporate features from multiple time points exhibit enhanced predictive power by capturing treatment dynamics.

A considerable portion radiomics research emphasizes feature extraction from subdivided regions of interest (ROI), such as intra- and peritumoral areas [17]. Although this method offers valuable insights, it introduces challenges in segmentation standardization and may not be easily generalizable across diverse clinical environments. There is an acknowledged necessity for models that utilize robust features extracted from the entire tumor volume, as this represents a more straightforward and clinically replicable segmentation task [19-21]. Our study proposes that employing an advanced multi-category feature selection strategy on the whole tumor ROI in pretreatment ultrasound can produce a highly predictive radiomics signature. We hypothesize that integrating this signature with essential clinicopathological factors into a nomogram will yield an enhanced, clinically applicable tool for individualized pathologic complete response (PCR) prediction in HER2-positive breast cancer, thereby eliminating the need for complex regional subdivision.

## 2 MATERIALS AND METHODS

### 2.1 Study Population and Design

This retrospective study received approval from the Institutional Review Boards of the participating academic medical centers, with the requirement for informed consent being waived. We conducted a screening of consecutive female patients diagnosed with primary, non-metastatic, HER2-positive invasive breast cancer who underwent neoadjuvant chemotherapy (NAC) followed by definitive surgery between January 2020 and December 2024.

The inclusion criteria encompassed: histologically confirmed HER2-positive invasive breast carcinoma, characterized by immunohistochemistry (IHC) scores of 3+ or 2+ with positive fluorescence in situ hybridization (FISH); completion of a standard NAC regimen incorporating trastuzumab, with or without pertuzumab; availability of high-quality pretreatment grayscale ultrasound (US) images in Digital Imaging and JPG format, conducted within four weeks prior to the initiation of NAC; and availability of a comprehensive pathological report from the surgical specimen for the assessment of pathological complete response (PCR).

The exclusion criteria included incomplete NAC cycles or surgeries performed at external institutions, as well as poor-quality US images with significant artifacts that impede accurate segmentation.

Using a computer-generated random number sequence, the cohort was stratified by institution and PCR status and subsequently divided into a training set (70%) for model development and an internal validation set (30%) for performance testing.

### 2.2 Treatment Evaluation and Pathological Evaluation

All patients were administered chemotherapy regimens based on anthracyclines and/or taxanes, in conjunction with anti-HER2 targeted therapy, in alignment with NCCN guidelines. The choice of specific regimen was determined by the treating oncologist. Upon completion of neoadjuvant chemotherapy (NAC), patients underwent either mastectomy or breast-conserving surgery, accompanied by sentinel lymph node biopsy or axillary lymph node dissection. The pathological evaluation of the surgical specimen was employed as the definitive standard for assessing treatment response. Pathological complete response (PCR) was rigorously defined as ypT0/Tis, indicating no residual invasive carcinoma in the breast, with the presence of ductal carcinoma in situ permitted, and ypN0, indicating no tumor deposits in any examined axillary lymph nodes. All pathology slides were independently reviewed by two specialized breast pathologists who were blinded to the imaging analyses and clinical data. Any discrepancies were resolved through a consensus review process.

### 2.3 Ultrasound Image Acquisition and Tumor Segmentation

Pre-treatment breast ultrasound examinations were conducted by experienced sonographers utilizing high-frequency linear array transducers (frequency range: 9-15 MHz) from major manufacturers (GE LOGIQ E9). Imaging parameters, including gain, depth, and focal zone, were optimized for each patient to ensure maximal lesion visibility. The imaging parameters, including gain, depth, and focal zone, were meticulously optimized for each patient to ensure maximal lesion conspicuity. The standard protocol entailed saving representative grayscale images in both longitudinal and transverse planes, capturing the largest tumor cross-section.

For image segmentation, all JPG images were anonymized and imported into ITK-SNAP 4.4. Careful attention was given to include all hypoechoic tumor tissue while excluding adjacent normal breast parenchyma, fat, and calcifications. To evaluate inter-observer reproducibility, a second radiologist (Reader 2) independently conducted the segmentation on 30 randomly selected cases from the entire cohort.

### 2.4 Radiomics Feature Extraction and Signature Construction

Radiomics feature extraction were performed using the Onekey AI, adhering to the Image Biomarker Standardization Initiative (IBSI) guidelines to ensure reproducibility.

**Feature Extraction:** From each segmented tumor region of interest (ROI), a comprehensive set of 1562 radiomic features was extracted. These features were systematically categorized into distinct groups: First-order Statistics: These are descriptors of the distribution of voxel intensities within the ROI, including metrics such as mean, median, 10th percentile, 90th percentile, entropy, kurtosis, and skewness.

Shape-based Features (2D): These features provide geometric descriptors of the ROI, encompassing measurements such as area, perimeter, major axis length, minor axis length, eccentricity, and solidity.

Texture Features: These features quantify intra-tumoral heterogeneity and are derived from various matrices, including: Gray-Level Co-occurrence Matrix (GLCM): Metrics such as contrast, correlation, energy, and homogeneity. Gray-Level Run Length Matrix (GLRLM): Metrics such as short-run emphasis, long-run emphasis, and run-length non-uniformity. Gray-Level Size Zone Matrix (GLSZM): Metrics such as zone entropy and size-zone non-uniformity. Gray-Level Dependence Matrix (GLDM): Metrics such as dependence entropy and dependence non-uniformity. Gray-Level Size Zone Matrix (GLSZM) metrics, such as zone entropy and size-zone non-uniformity, and Gray-Level Dependence Matrix (GLDM) metrics, including dependence entropy and dependence non-uniformity, were analyzed.

**Feature preprocessing and selection:** Feature preprocessing and selection involved a meticulous multi-step procedure applied exclusively to the training cohort to mitigate risks of data leakage and overfitting.

Stability filtering: features with an inter-observer intraclass correlation coefficient (ICC) below 0.90, based on 30 double-segmented cases were excluded to ensure robustness.

**Variance and correlation filtering:** features exhibiting near-zero variance (variance  $< 0.01$ ) were removed. Subsequently, features with high correlation (absolute Pearson correlation coefficient  $> 0.95$ ) were identified, and from each cluster of correlated features, the feature with the highest mean absolute correlation to others was retained.

Predictive feature selection: the remaining features underwent standardization through z-score normalization, followed by a two-stage selection process.

The Least Absolute Shrinkage and Selection Operator (LASSO) regression, utilizing 10-fold cross-validation, was employed to reduce coefficients and select a subset of non-redundant features predictive of pathological complete response (PCR). Subsequently, Recursive Feature Elimination (RFE) based on a Support Vector Machine (SVM) classifier was conducted on the features selected by LASSO to determine the most optimal and parsimonious feature set.

**Radiomics Signature (Rad-score) Building:** the final selected features were assigned weights according to their coefficients obtained from a logistic regression model fitted to the training dataset. The Rad-score for each patient was computed as a linear combination of these selected feature values and their corresponding weights.

## 2.5 Clinical Model and Combined Nomogram

Clinicopathological data were extracted from electronic medical records, encompassing variables such as age, menopausal status, clinical T and N stage (according to the AJCC 8th edition), histological grade, and biomarker status (estrogen receptor [ER], progesterone receptor [PR], and Ki-67 index). Univariate logistic regression analysis was performed to identify clinical factors significantly associated with PCR within the training cohort. In the multivariate logistic regression analysis, variables with a P-value less than 0.05 were identified as independent predictors and subsequently utilized to construct a clinical-only prediction model. The final predictive nomogram was developed by integrating the Rad-score with the independent clinical predictors into a multivariable logistic regression model within the training cohort.

## 2.6 Model Evaluation and Statistical Analysis

The efficacy of the radiomics signature, the clinical model, and the combined nomogram was assessed in both the training and independent validation cohorts.

**Discrimination:** The primary metric was the area under the receiver operating characteristic curve (AUC). Differences in AUC between models were compared using DeLong's test.

**Calibration:** The agreement between predicted probabilities and observed outcomes was assessed using calibration plots and the Hosmer-Lemeshow goodness-of-fit test, where a non-significant P-value greater than 0.05 indicates good calibration.

**Clinical Utility:** Decision curve analysis (DCA) was conducted to determine the net benefit of each model across a spectrum of threshold probabilities, thereby quantifying their clinical value in comparison to PCR or NO PCR strategies.

All statistical analyses were performed using Onekey AI software. A two-sided P value  $< 0.05$  was considered statistically significant.

## 3 RESULTS

### 3.1 Patient Characteristics

The baseline demographic and clinicopathological characteristics of the 158 patients are summarized (Table 1). The overall PCR rate was 56.33% (89 out of 158). There were no significant differences in baseline characteristics between the training and validation sets (all  $P > 0.05$ ).

**Table 1** Baseline Characteristics of Patients in the Training and Validation Cohorts

| Characteristic             | Total Cohort (n=158) | Validation Cohort (n=48) | Train Cohort (n=110) | P-value |
|----------------------------|----------------------|--------------------------|----------------------|---------|
| Age (years), mean $\pm$ SD | 52.418 $\pm$ 8.507   | 53.667 $\pm$ 9.217       | 51.873 $\pm$ 8.162   | 0.224   |
| Clinical T Stage, n (%)    |                      |                          |                      | 0.727   |
| cT1-2                      | 124(78.481)          | 39(81.250)               | 85(77.273)           |         |
| cT3-4                      | 34(21.519)           | 9(18.750)                | 25(22.727)           |         |
| Clinical N Stage, n (%)    |                      |                          |                      | 0.218   |
| cN0                        | 38(24.051)           | 8(16.667)                | 30(27.273)           |         |
| cN+                        | 120(75.949)          | 40(83.333)               | 80(72.727)           |         |
| ER Status, n (%)           |                      |                          |                      | 0.572   |
| Positive                   | 72(45.570)           | 24(50.000)               | 48(43.636)           |         |
| Negative                   | 86(54.430)           | 24(50.000)               | 62(56.364)           |         |
| PR Status, n (%)           |                      |                          |                      | 0.391   |
| Positive                   | 89(56.329)           | 30(62.500)               | 59(53.636)           |         |
| Negative                   | 69(43.671)           | 18(37.500)               | 51(46.364)           |         |
| Clinical ALL Stage         |                      |                          |                      | 0.69    |
| I1-2                       | 104(65.823)          | 30(62.500)               | 74(67.273)           |         |
| 3-4                        | 54(34.177)           | 18(37.500)               | 36(32.727)           |         |
| PCR Status, n (%)          |                      |                          |                      | 0.604   |
| PCR                        | 89(56.329)           | 30(62.500)               | 59(53.636)           |         |
| Non-PCR                    | 69(43.671)           | 18(37.500)               | 51(46.364)           |         |

### 3.2 Radiomics Feature Selection and model Performance

Following variance and correlation filtering, 15 features were retained for predictive selection. The LASSO-RFE pipeline selected 10 optimal features for the final signature, originating from first-order statistics and texture matrices (Figure 1), highlighting the importance of both intensity distribution and complex spatial heterogeneity patterns within the tumor. The radiomics signature showed good and stable predictive performance, with max AUC of 0.717 (95% CI: 0.66-0.81) in the training cohort and 0.705 (95% CI: 0.56-0.85) in the validation cohort in MLP model (Table 2).

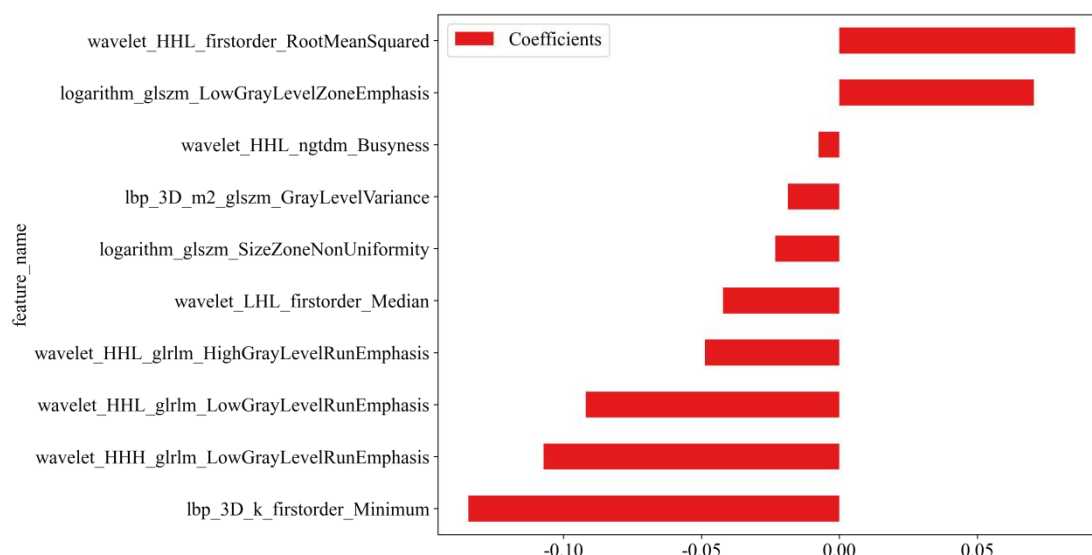


**Figure 1** Features Coefficients of Patients in the Training and Validation Cohorts

**Table 2** Model predictions of Radiomics in the Training and Validation Cohorts

| Model            | Cohort     | AUC (95% CI) |                   | Sensitivity | Specificity | Accuracy |
|------------------|------------|--------------|-------------------|-------------|-------------|----------|
| LR               | train      | 0.800        | (0.7189-0.8812)   | 0.717       | 0.754       | 0.736    |
|                  | Validation | 0.526        | (0.3557 - 0.6954) | 0.407       | 0.714       | 0.542    |
| NaiveBayes       | train      | 0.693        | (0.5952 - 0.7904) | 0.925       | 0.404       | 0.655    |
|                  | Validation | 0.651        | (0.4937 - 0.8079) | 0.852       | 0.429       | 0.667    |
| SVM              | train      | 0.762        | (0.6745 - 0.8501) | 0.623       | 0.772       | 0.700    |
|                  | Validation | 0.543        | (0.3751 - 0.7113) | 0.370       | 0.857       | 0.583    |
| KNN              | train      | 0.770        | 0.6857 - 0.8545   | 0.717       | 0.684       | 0.700    |
|                  | Validation | 0.547        | 0.3820 - 0.7115   | 0.593       | 0.571       | 0.583    |
| RandomForest     | train      | 0.881        | 0.8180 - 0.9440   | 0.925       | 0.702       | 0.809    |
|                  | Validation | 0.436        | (0.2669 - 0.6044) | 0.296       | 0.905       | 0.562    |
| ExtraTrees       | train      | 0.964        | (0.9355 - 0.9930) | 0.981       | 0.825       | 0.900    |
|                  | Validation | 0.529        | (0.3612 - 0.6970) | 0.593       | 0.571       | 0.583    |
| XGBoost          | train      | 0.959        | (0.9252 - 0.9927) | 0.943       | 0.860       | 0.900    |
|                  | Validation | 0.441        | (0.2723 - 0.6095) | 0.185       | 0.952       | 0.521    |
| LightGBM         | train      | 0.661        | (0.5799 - 0.7429) | 0.849       | 0.474       | 0.655    |
|                  | Validation | 0.397        | (0.2633 - 0.5304) | 1.000       | 0.000       | 0.562    |
| GradientBoosting | train      | 1.000        | (1.0000 - 1.0000) | 1.000       | 1.000       | 1.000    |
|                  | Validation | 0.594        | (0.4312 - 0.7575) | 0.333       | 0.952       | 0.604    |
| AdaBoost         | train      | 0.934        | (0.8923 - 0.9763) | 0.755       | 0.965       | 0.864    |
|                  | Validation | 0.587        | (0.4239 - 0.7507) | 0.667       | 0.524       | 0.604    |

| Model | Cohort     | AUC (95% CI)            | Sensitivity | Specificity | Accuracy |
|-------|------------|-------------------------|-------------|-------------|----------|
| MLP   | train      | 0.717 (0.6220 - 0.8113) | 0.660       | 0.702       | 0.682    |
|       | Validation | 0.705 (0.5584 - 0.8526) | 0.556       | 0.810       | 0.667    |

### 3.3 Development and Performance of the Clinical Model and Final Nomogram

Multivariate logistic regression analysis identified PR negativity (Odds Ratio [OR]: -0.606, 95% CI: -1.088-[-10.124],  $P=0.039$ ) as independent clinical predictors of PCR. This combined model achieved the highest discriminatory ability, with an AUC of 0.749(0.659 - 0.839) in the training cohort and 0.744(0.605 - 0.884) in the validation cohort (Table 3, Figure 2). The final nomogram integrated the Rad-score with PR status (Figure 3). The nomogram's performance was significantly superior to that of the clinical-only model (DeLong's test,  $P<0.001$  in validation) and showed a strong trend towards improvement over the radiomics-only model.

**Table 3** Predictive Performance of Different Models in the Training and Validation Cohorts

| Model     | Cohort     | AUC (95% CI)           | Sensitivity | Specificity | Accuracy |
|-----------|------------|------------------------|-------------|-------------|----------|
| Clinic    | Train      | 0.620(0.5284-0.7109)   | 0.660       | 0.579       | 0.618    |
| Radiomics | Train      | 0.717(0.6220-0.8113)   | 0.660       | 0.702       | 0.682    |
| Combined  | Train      | 0.749(0.6589-0.8386)   | 0.849       | 0.526       | 0.682    |
| Clinic    | Validation | 0.675(0.5399 - 0.8093) | 0.778       | 0.571       | 0.688    |
| Radiomics | Validation | 0.705(0.5584 - 0.8526) | 0.556       | 0.810       | 0.667    |
| Combined  | Validation | 0.744(0.6046 - 0.8840) | 0.593       | 0.810       | 0.688    |

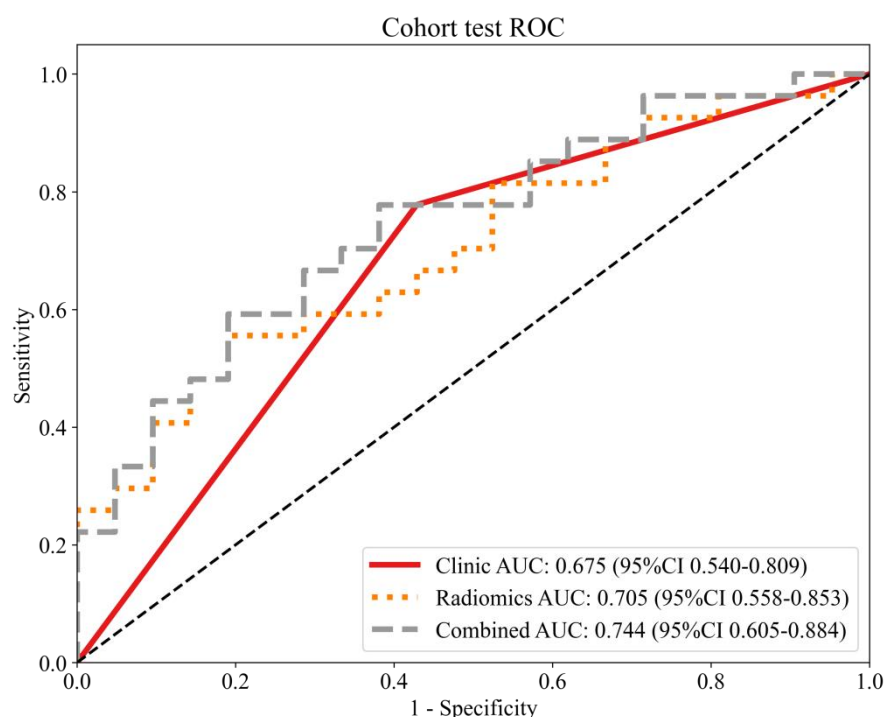


**Figure 2** ROC of Patients in the Training and Validation Cohorts

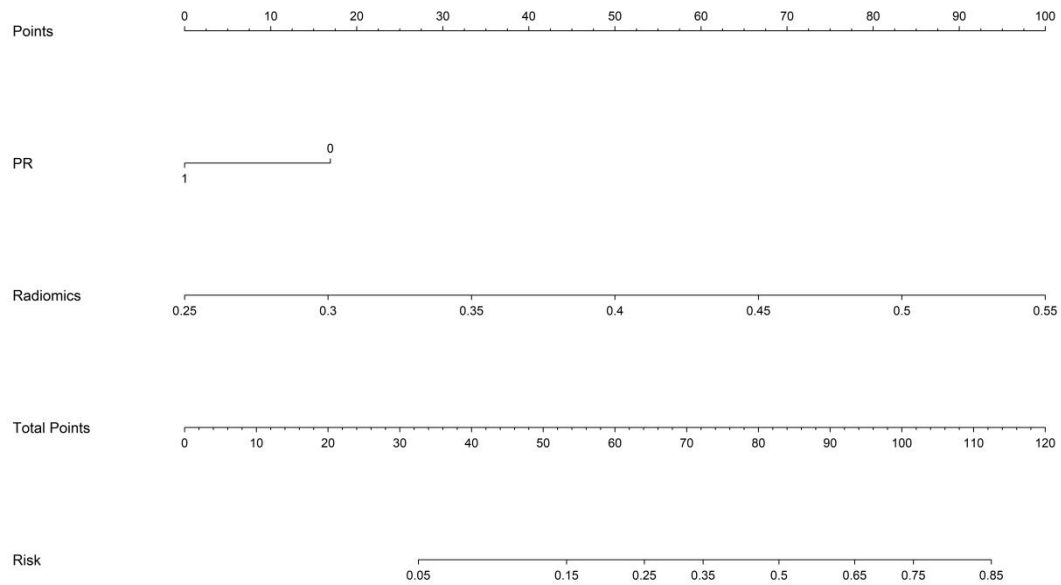


**Figure 3** Nomogram of Patients in the Training and Validation Cohorts

Decision Curve Analysis (DCA) indicated that utilizing the nomogram for clinical decision-making offered a higher net benefit compared to the "treat-all" or "treat-none" strategies over a broad spectrum of clinically reasonable threshold probabilities (Figure 4). The calibration curve for the nomogram exhibited a strong concordance with the ideal 45-degree line in both the training and validation cohorts (Figure 5).

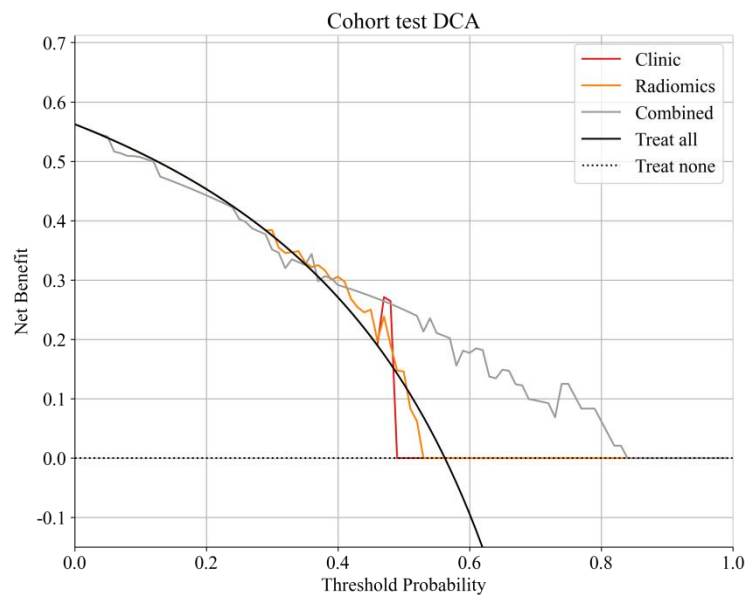


**Figure 4** DCA of Patients in the Training and Validation Cohorts

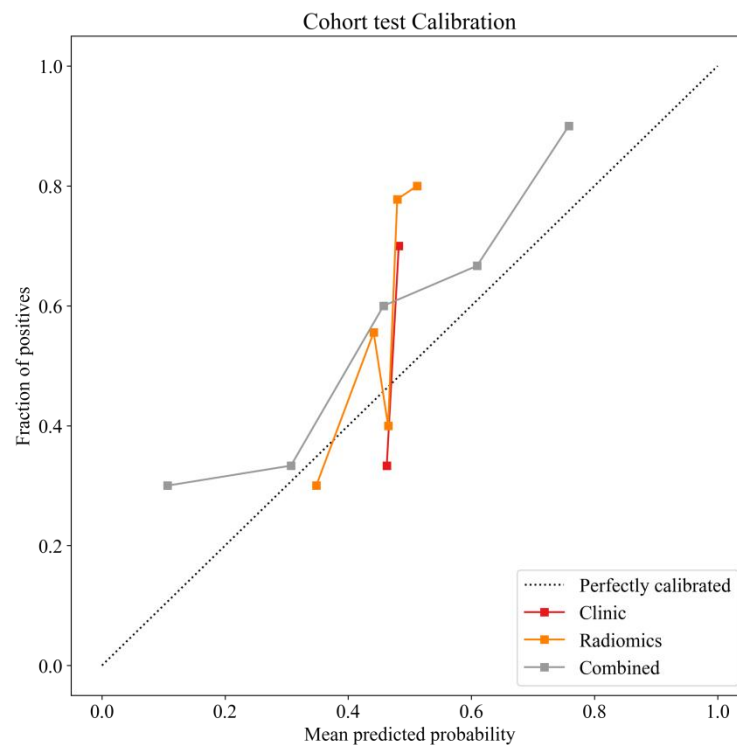


**Figure 5** Calibration Curve in the Training and Validation Cohorts

#### 4 DISCUSSION

In this retrospective study, we developed and validated a pretreatment ultrasound-based radiomics nomogram for the individualized prediction of pathological complete response (PCR) to neoadjuvant chemotherapy (NAC) in patients with HER2-positive breast cancer. Our model is based on a sophisticated selection of radiomics features extracted from the entire tumor volume, integrated with key clinical biomarkers. The final nomogram demonstrated predictive accuracy, good calibration, and favorable clinical utility, indicating its potential as a practical tool for personalizing NAC strategies.

The success of our model is rooted in the multi-step, rigorous feature engineering process applied to the whole-tumor region of interest (ROI). The selected 10-feature signature comprises a combination of first-order intensity statistics and higher-order texture features. This is consistent with the biological understanding that tumors with high internal heterogeneity, often indicative of genomic instability and clonal diversity, may exhibit differential responses to therapy [4-13]. Our approach illustrates that meaningful predictive information can be effectively captured from the global tumor phenotype without necessitating complex subdivision of the ROI, potentially enhancing the method's clinical translatability and reproducibility across different institutions and operators [14-17].

The integration of the radiomics signature with progesterone receptor (PR) has resulted in the development of a robust multi-parametric predictive tool. Progesterone receptor (PR) is well-recognized indicators of a more aggressive and proliferative tumor biology, which is typically more responsive to cytotoxic chemotherapy. This aligns with their roles as independent predictors within our model [18-19]. The nomogram effectively combines these established clinical biomarkers with the novel, quantitative imaging phenotype provided by radiomics. This integration likely captures a more comprehensive view of the tumor, encompassing both its molecular characteristics (via PR) and its macroscopic phenotypic expression (via radiomics), thereby leading to enhanced predictive performance compared to the use of either component in isolation [20].

The clinical implications of our findings are significant. An accurate pretreatment prediction model could profoundly influence patient management in the neoadjuvant setting. For patients predicted to have a very high likelihood of achieving a pathologic complete response (PCR), clinicians might consider exploring strategies within clinical trial frameworks, such as evaluating de-escalated chemotherapy regimens or shorter treatment durations. The objective is to minimize both acute and long-term toxicity without compromising oncologic outcomes [2-13]. In contrast, for patients predicted to be non-responders, early treatment intensification may be considered. This could involve the initial incorporation of novel antibody-drug conjugates, such as trastuzumab deruxtecan, dual HER2 blockade with pertuzumab if not previously utilized, or participation in clinical trials exploring new targeted agents or immunotherapy combinations [12-16]. Such a risk-adapted strategy exemplifies the principles of precision oncology.

Our study has several limitations that merit consideration. Firstly, the retrospective design may introduce inherent selection bias. Secondly, although we conducted internal validation, external validation in a larger, prospective, and multinational cohort is crucial to confirm the generalizability and robustness of our nomogram. Thirdly, our model is based on two-dimensional ultrasound images. The utilization of three-dimensional automated breast ultrasound (ABUS) could offer more comprehensive volumetric feature extraction. Fourth, we concentrated on predicting outcomes before



treatment. By incorporating serial ultrasound imaging during treatment to analyze delta-radiomics, which involves changes in features over time, we could capture dynamic response patterns and improve prediction accuracy, as suggested by recent research. Future studies should also consider integrating ultrasound radiomics with other data types, such as MRI radiomics or circulating tumor DNA, to create a more comprehensive multi-omics predictive profile.

## 5 CONCLUSION

We have developed and validated a pretreatment ultrasound-based radiomics nomogram that effectively predicts the likelihood of achieving a complete response following neoadjuvant chemotherapy in HER2-positive breast cancer patients. By using a thorough whole-tumor feature selection strategy and combining the resulting radiomics signature with key clinical biomarkers, this non-invasive tool offers individualized risk assessment with high accuracy. It represents a practical step towards personalized neoadjuvant therapy, potentially guiding clinical decisions by identifying patients who may benefit from treatment de-escalation or early intensification, ultimately aiming to improve therapeutic efficacy and patient quality of life.

## COMPETING INTERESTS

The authors have no relevant financial or non-financial interests to disclose.

## FUNDING

This work was supported by the Science and Technology Program of Shaoguan City (No. 210922204531943, No. 230330098033759), Medical Science and Technology Research Fund Project of Guangdong Province (No. B2023468), and Health Research Project of Shaoguan City (No. Y22103, No. Y2023080).

## REFERENCES

- [1] Wagle NS, Nogueira L, Devasia TP, et al. Cancer treatment and survivorship statistics. *CA: A Cancer Journal for Clinicians*, 2025, 75(4): 308-340.
- [2] Bardia A, Jhaveri K, Im SA, et al. Datopotamab Deruxtecan Versus Chemotherapy in Previously Treated Inoperable/Metastatic Hormone Receptor-Positive Human Epidermal Growth Factor Receptor 2-Negative Breast Cancer: Primary Results From TROPION-Breast01. *Journal of Clinical Oncology*, 2025, 43(3): 285-296.
- [3] Gillies R J, Kinahan P E, Hricak H, et al. Radiomics: Images Are More than Pictures, They Are Data. *Radiology*. 2016, 278(2): 563-577.
- [4] Lin Z, Zheng M, Li Z, et al. Development and validation of a delta ultrasomics model for predicting treatment response to neoadjuvant chemotherapy in breast cancer. *Translational Cancer Research*, 2025, 14(11): 7967-7979.
- [5] Moore-Palhares D, Alberico D, Chan AW, et al. Quantitative ultrasound imaging for predicting response and guiding personalized neoadjuvant chemotherapy in breast cancer: randomized phase 2 clinical trial results. *NPJ Precision Oncology*, 2025, 9(1): 390.
- [6] Liu J, Leng X, Yuan Z, et al. Predicting breast cancer response to neoadjuvant chemotherapy with ultrasound-based deep learning radiomics models -- dual-center study. *BMC Cancer*, 2025, 25(1): 1737.
- [7] Wang M, Huang Z, Tian H, et al. Longitudinal Ultrasound Delta Radiomics for Early Stratified Prediction of Tumor Response to Neoadjuvant Chemotherapy in Breast Cancer. *Academic Radiology*, 2025, 32(12): 7119-7133.
- [8] Peng Q, Ji Z, Xu N, et al. Prediction of neoadjuvant chemotherapy efficacy in patients with HER2-low breast cancer based on ultrasound radiomics. *Cancer Imaging*, 2025, 25(1): 112.
- [9] Wei C, Jia Y, Gu Y, et al. Predictive Analysis of Neoadjuvant Chemotherapy Efficacy in Breast Cancer Using Multi-Region Ultrasound Imaging Features Combined With Pathological Parameters. *Ultrasound in Medicine and Biology*, 2025, 51(12): 2205-2216.
- [10] Moore-Palhares D, Sannachi L, Chan AW, et al. Validation of a Quantitative Ultrasound Texture Analysis Model for Early Prediction of Neoadjuvant Chemotherapy Response in Breast Cancer: A Prospective Serial Imaging Study. *Cancers (Basel)*, 2025, 17(15): 2594.
- [11] Liu J, Xue X, Yan Y, et al. Prediction of breast cancer HER2 status changes based on ultrasound radiomics attention network. *Computer Methods and Programs in Biomedicine*, 2025, 271: 108987.
- [12] Valizadeh P, Jannatdoust P, Moradi N, et al. Ultrasound-based machine learning models for predicting response to neoadjuvant chemotherapy in breast cancer: A meta-analysis. *Clinical Imaging*, 2025, 125: 110574.
- [13] Chen M, Hong T, Wang Y, et al. Effect of a machine learning prediction model on the false-negative rate of sentinel lymph node biopsy for clinically node-positive breast cancer after neoadjuvant chemotherapy. *Breast*, 2025, 83: 104543.
- [14] Tenghui W, Xinyi L, Ziyi S Y, et al. Combination of ultrasound-based radiomics and deep learning with clinical data to predict response in breast cancer patients treated with neoadjuvant chemotherapy. *Frontiers in Oncology*, 2025, 15: 1525285.
- [15] Zhang H, Lang M, Shen H, et al. Machine learning-based fusion model for predicting HER2 expression in breast cancer by Sonazoid-enhanced ultrasound: a multicenter study. *Frontiers of Medicine (Lausanne)*, 2025, 12: 1585823.

- [16] Fan Y, Sun K, Xiao Y, et al. Deep learning predicts HER2 status in invasive breast cancer from multimodal ultrasound and MRI. *Biomolecules and Biomedicine*, 2025, 25(10): 2243-2251.
- [17] Yao J, Zhou W, Jia X, et al. Machine learning prediction of pathological complete response to neoadjuvant chemotherapy with peritumoral breast tumor ultrasound radiomics: compare with intratumoral radiomics and clinicopathologic predictors. *Breast Cancer Research and Treatment*, 2025, 212(2): 325-336.
- [18] Chan AW, Sannachi L, Moore-Palhares D, et al. Validation of Quantitative Ultrasound and Texture Derivative Analyses-Based Model for Upfront Prediction of Neoadjuvant Chemotherapy Response in Breast Cancer. *Journal of Imaging*, 2025, 11(4): 109.
- [19] Feng X, Shi Y, Wu M, et al. Predicting the efficacy of neoadjuvant chemotherapy in breast cancer patients based on ultrasound longitudinal temporal depth network fusion model. *Breast Cancer Research*, 2025, 27(1): 30.
- [20] Zhou P, Qian H, Zhu P, et al. Machine learning for predicting neoadjuvant chemotherapy effectiveness using ultrasound radiomics features and routine clinical data of patients with breast cancer. *Frontiers in Oncology*, 2025, 14: 1485681.
- [21] Xie J, Wei J, Shi H, et al. A deep learning approach for early prediction of breast cancer neoadjuvant chemotherapy response on multistage bimodal ultrasound images. *BMC Med Imaging*, 2025, 25(1): 26.